Modeling of surface metrology of state-of-the-art x-ray mirrors as a result of stochastic polishing process

Valeriy V. Yashchuk,*[,1] Yury N. Tyurin,[2,3] and Anastasia Y. Tyurina[3]
[1]Lawrence Berkeley National Laboratory, Berkeley, California 94720, USA
[2]Moscow State University, Moscow, Russia
[3]Second Star Algonumerics, Needham, MA 02494, USA

ABSTRACT

The design and evaluation of the expected performance of new optical systems requires sophisticated and reliable information about the surface topography for planned optical elements before they are fabricated. The problem is especially severe in the case of x-ray optics for modern diffraction-limited-electron-ring and free-electron-laser x-ray facilities, as well as x-ray astrophysics missions, such as the X-ray Surveyor under development. Modern x-ray source facilities are reliant upon the availability of optics of unprecedented quality, with surface slope accuracy < 0.1μrad. The unprecedented high angular resolution and throughput of future x-ray space observatories require high quality optics of hundreds square meters in total area. The uniqueness of the optics and limited number of proficient vendors makes the fabrication extremely time consuming and expensive, mostly due to the limitations in accuracy and measurement rate of metrology used in fabrication. In this work we continue investigating the possibility to improve metrology efficiency via comprehensive statistical treatment of a compact volume of metrology data, considered to be a result of a stochastic polishing process. If successful, the modeling could provide a feedback to deterministic polishing processes, avoiding time-consuming, whole scale metrology measurements over the entire optical surface with the resolution required to cover the entire desired spatial frequency range. The modeling also allows forecasting metrology data for optics made by the same vendor and technology. The forecast data is vital for reliable specification for optical fabrication, evaluated from numerical simulation to be exactly adequate for the required system performance, avoiding both over- and under-specification.

Keywords: surface metrology, time-invariant linear filter, TILF, autoregressive moving average, ARMA, power spectral density, PSD, fabrication tolerances, x-ray optics, surface slope profilometry

1. INTRODUCTION

The design and evaluation of the expected performance of new optical systems requires sophisticated and reliable information about the surface topography for planned optical elements before they are fabricated. The problem is especially severe in the case of x-ray optics for modern diffraction-limited-electron-ring and free-electron-laser x-ray source facilities, as well as x-ray astrophysics missions under development. The modern x-ray source facilities are reliant upon the availability of x-ray optics of unprecedented quality, with surface slope accuracy better than 0.1 μrad and surface height error of less than 1 nm.[1-5] The unprecedented high angular resolution and throughput of future x-ray space observatories, such as the X-Ray Surveyor mission,[6] require high quality optics of hundreds square meters in total area. The uniqueness of the optics and limited number of proficient vendors makes the fabrication extremely time consuming and expensive, mostly due to the limitations in accuracy and measurement rate of the available metrology.

Recently, a possibility to improve metrology efficiency via comprehensive statistical treatment of a compact volume of metrology data has been suggested (see Refs.[7-9] and references therein). It has been demonstrated[8,9] that one-dimensional (1D) slope metrology with super polished x-ray mirrors can be treated as a result of a stochastic polishing process. In this case, autoregressive-moving-average (ARMA) and an extension of ARMA to time-invariant linear filter (TILF) modeling[10,11] allows a high degree of confidence when fitting the metrology data with a limited number of parameters.

With the parameters of the determined model, the surface slope profiles of the prospective (before fabrication) optics, made by the same vendor and technology, can be forecast. The forecast data is vital for reliable specification for optical

*vvyashchuk@lbl.gov; phone 1 510 495-2592; fax 1 510 486-7696; www-esg.lbl.gov/Production/OML/index.html

fabrication, evaluated from numerical simulation to be necessary and sufficient for the required system performance, avoiding both over- and under-specification.[12-13]

Considering surface slope metrology data to be the results of a stationary stochastic polishing process and using a compact volume of metrology data, modeling can be utilized to provide feedback to deterministic optical polishing. This can avoid time-consuming whole scale metrology measurements over the entire optical surface with the resolution required to cover the entire spatial frequency range, important for the optical system performance.

In the present work, we continue investigations, started in Refs.[8-13] First, we briefly review the mathematical fundamentals of 1D ARMA modeling of topography of random rough surfaces (Sec. 2). In Sec. 3, we analyze a generalization of ARMA modeling with TILF approach. We analytically show that the suggested symmetric TILF approximation has all advantages of one-sided AR and ARMA modeling, but it additionally has improved fitting accuracy. It is free of the causality problem, which can be thought of as a limitation of ARMA modeling of surface metrology data. A new algorithm for identification of an optimal, symmetric TILF model with a minimum number of parameters and smallest residual error is derived in Sec. 4. Finally, in Sec. 5 we verify the efficiency of the developed algorithm in application to modeling of a series of stochastic processes, which are generated with the known ARMA model, determined for surface slope data for a state-of-the-art x-ray mirror. The paper concludes (Sec. 6) by summarizing the main concepts discussed throughout the paper and stating a plan for extending the suggested approach to parameterize the results of 2D surface metrology data.

2. ONE DIMENSIONAL STATISTICAL MODELING AND FORECASTING OF RANDOM ROUGH SURFACES

2.1 A brief review of ARMA modeling

Let us consider the surface slope metrology of high quality x-ray optics. For the one dimensional case, the result of the metrology is a distribution (trace) of residual (after subtraction of the best fit figure and trends) slopes $X[n]$ measured over discrete points $x_n = n \cdot \Delta x$ [$n = 1, ..., N$, where N is the total number of observations, and $(N-1)\Delta x$ is the total length of the trace], uniformly, with an increment Δx, distributed along the trace.

ARMA modeling describes the discrete surface slope distribution $\alpha[n]$ as a result of a uniform stochastic process:[14,15]

$$X[n] = \sum_{l=1}^{p} a_l X[n-l] + \sum_{l=0}^{q} b_l \nu[n-l], \tag{1}$$

where $\nu[n]$ is zero-mean unit-variance white Gaussian noise (referred to as 'white Gaussian noise') that is the driving noise of the model. The parameters p and q are the orders of the autoregressive and moving average processes, respectively. At $q = 0$ and $b_0 = 1$, the ARMA process (1) reduces to an AR stochastic process. Additional to the linearity, the ARMA transformation is time-invariant since its coefficients depend on the relative lags, l, rather than on n. The goal of the modeling is to determine the ARMA orders and estimate the corresponding AR and MA coefficients a_l and b_l.[16-18]

Due to the availability of sophisticated statistical software capable for ARMA modeling of experimental data, ARMA fitting becomes a rather routine task of finding the ARMA model parameters and verifying the statistical reliability of the model. We use a commercially available software package EViews 8.[19] In particular, the software provides easy-to-use ARMA modeling tools oriented to econometric analysis, forecasting, and simulation.

ARMA fitting allows for replacement of the spectral estimation problem with a problem of parameter estimation. In principle, the parameters of a successful ARMA model for a rough surface should relate to the polishing process. The analytical derivation of such relation is a separate difficult task; there are just a few works that try to solve this problem.[20,21] Instead, most of the existing work provides an empirical ARMA description for the results from polishing processes.[16,22] When an ARMA model is identified, the corresponding power spectral density (PSD) distribution can be analytically derived:[14]

$$P_X(f) = \sigma^2 \frac{B[e^{i2\pi f}]B[e^{-i2\pi f}]}{A[e^{i2\pi f}]A[e^{-i2\pi f}]}, \tag{2}$$

where the frequency $f \in [-0.5, 0.5]$,

$$A[e^{i2\pi f}] = 1 + a_1 e^{i2\pi f} + \ldots + a_p e^{i2\pi p f}, \tag{3}$$

$$B[e^{i2\pi f}] = b_0 + b_1 e^{i2\pi f} + \ldots + b_q e^{i2\pi q f}. \tag{4}$$

Equation (2) can be expressed as

$$P_X(f) = \sigma^2 \frac{(b_0 + b_1 z^{-1} + \ldots + b_q z^{-q})(b_0 + b_1 z^{1} + \ldots + b_q z^{q})}{(1 - a_1 z^{-1} - \ldots - a_p z^{-p})(1 - a_1 z^{1} - \ldots - a_p z^{p})}, \tag{5}$$

where $z = e^{i2\pi f}$ and σ^2 is the variance of the driving noise $\nu[n]$.

Therefore, a low-order ARMA fit, if successful, allows parametrization of both the PSD and the ACF of a random rough surface. As a result, the PSD distributions appear as highly smoothed versions of the corresponding estimates via a direct digital Fourier transform (DFT).[8,9] Description of a rough surface as the result of an ARMA stochastic process provides a model-based mechanism for extrapolating the spectra outside the measured bandwidth.[8,9]

Trustworthy ARMA modeling and forecasting based on a limited number of observations assumes statistical stability of the data used. The data are statistically stable if they are the result of a so called wide sense stationary (WSS) random process (see, for example, Ref.[14]). The process $X[n]$, where $n = 1, .., N$, and N is the number of observations, is a WSS process if its auto-covariance function (ACF),

$$r_X[l] = E(X[n]X[n-l]), \tag{6}$$

depends only on the lag l, and does not depend on the value of n. In (1) E is the expectation operator. Note that the PSD of the WSS random process $X[n]$ can be found from the ACF [compare to Eqs. (2) and (5)]:

$$P_X(f) = \sum_{l=-\infty}^{\infty} r_X[l] e^{-i2\pi l f} = \sum_{l=-\infty}^{\infty} r_X[l] z^{-l}. \tag{7}$$

According to Eq. (5), $r_X[l]$ is a nonlinear function of the ARMA coefficients, a_l for $l = 1, ..., p$ and b_l for $l = 1, ..., q$.

Recent publications[8,9] describe a successful application of ARMA modeling to the experimental surface slope data for a 1280 m spherical reference mirror.[23,24] The data was obtained with the Advanced Light Source (ALS) Developmental Long Trace Profiler (DLTP)[25] and verified in cross-comparison with measurements performed with the HZB/BESSY-II Nanometer Optical Component Measuring machine (NOM),[26-29] one of the world's best slope measuring instruments.

2.2 TILF approach to solve causality problem of ARMA modeling

With the obvious success and perspective of the application of 1D ARMA modeling to 1D surface slope metrology, the inherent causality of the modeling is thought of as a limiting factor that also complicates extension of the method to modeling 2D surface metrology available, for example, with high precision interferometers and microscopes.

Indeed, ARMA modeling is inherently causal, assuming that the current value of the process depends only upon the past, as expressed with Eq. (1). While in the case of time series, the property of causality is natural, in the case of modeling of surface metrology data, the causality can be thought of as a limitation. A valid model should describe the reversed surface metrology data corresponding to the measurements with the optic rotated (flipped) by 180 degrees with respect to the scanning direction of the profiler. The direct and reversed residual slope traces are related through a straightforward transformation of the coordinate system and change to the opposite sign of the measured slope values (see, for example, Ref.[7]).

In our previous work,[10,11] we have suggested a simple way of fixing the causality problem in ARMA modeling.

First, let us note that ARMA modeling of the direct and reversed residual slope traces effectively establishes, for each other, a relation between the current slope element $X[n]$ and the 'future' ones, $X[n+l]$ and $\nu[n+l]$ [compare with Eq. (1)] with positive, rather than negative, lag value:

$$X[n] = \sum_{l=1}^{p} a_l^* X[n+l] + \sum_{l=0}^{q} b_l^* \nu[n+l], \tag{8}$$

where for the direct slope trace $X[n]$, a_l^* and b_l^* denote the ARMA parameters determined by modeling of the reversed trace. The causality limitation is solved by a straightforward merging of the causal stochastic processes (1) and (8) to a 'two-sided symmetrical ARMA' model of the 1D slope trace:

$$X[n] = \frac{1}{2}\left\{ \sum_{l=1}^{p} \left(a_l^* X[n+l] + a_l X[n-l] \right) + \sum_{l=0}^{q} \left(b_l^* \nu[n+l] + b_l \nu[n-l] \right) \right\}. \tag{9}$$

Unlike causal, one-sided ARMA modeling, the 'two-sided symmetrical ARMA' model, depicted with Eq. (9), is free of the limitation of the fixed direction (time flow) and causation. This implies that the current value of the surface slope depends upon the past and the future that is, in our case, the neighboring points with the positive and negative lag values. Such an extension of AR modeling closely relates to the time-invariant linear filter approach.[29]

The TILF approximation has all the advantages of one-sided AR and ARMA modeling.[10,11] The TILF approach, which is basically free of causality limitation, naturally includes a 'two-sided symmetrical ARMA' model that overcomes the causality problem in the framework of ARMA modeling. In Sec. 3, we provide a brief introduction to TILF theory in application to modeling of surface metrology data.

3. TIME-INVARIANT LINEAR FILTERS IN APPLICATION TO MODELING OF SURFACE METROLOGY

3.1 A brief review of TILF mathematical foundations

For the one dimensional case, the time-invariant linear filter C with weights $\{c_i, i = 0, \pm 1, ...\}$ is a linear operator that transforms one stochastic process $\{X[t], t = 0, \pm 1, ...\}$ into another (filtered) process $\{Y[t], t = 0, \pm 1, ...\}$:[10,11,29]

$$Y[t] = \sum_{l=-\infty}^{\infty} c_l X[t-l] \equiv C * X[t]. \tag{10}$$

Similar to the ARMA transformation, the TILF C is linear and time-invariant. The filter C possesses the property of causality if

$$c_i = 0 \quad \text{for} \quad i < 0. \tag{11}$$

The requirement of stability of the transformation implies that the filter is absolutely summable:

$$\sum_{l=-\infty}^{\infty} |c_l| < \infty. \tag{12}$$

Also similar to ARMA modeling, when an optimal TILF is identified, the corresponding power spectral density distribution can be analytically derived [compare with Eq. (5)]:

$$P_Y(f) = \left| \sum_{l=-\infty}^{\infty} c_l \, e^{i2\pi l f} \right|^2 P_X(f). \tag{13}$$

Almost any ARMA process $X[t]$ with the parameters p and q can be obtained from white Gaussian noise $\nu[t]$ by application of the corresponding casual TILF:[29]

$$X[t] = \sum_{l=0}^{\infty} c_l \, \nu[t-l]. \tag{14}$$

The weights c_l in (14) are determined by the relation:

$$\sum_{l=0}^{\infty} c_l \, z^l = b(z)/a(z), \quad |z| \le 1, \tag{15}$$

where the AR and MA polynomials in the right hand side of Eq. (15) are, respectively,

$$a(z) = 1 - a_1 z^1 - \ldots - a_p z^p \text{ and } b(z) = 1 + b_1 z^1 + \ldots + b_q z^q. \tag{16}$$

Consequently, 'two-sided ARMA' process given with Eq. (9), can be expressed via a TILF in the form of Eq. (9), which is free of the causality limitation:

$$X[t] = \frac{1}{2}\left\{ \sum_{l=0}^{\infty} c_l \, \nu[t-l] + \sum_{l=0}^{\infty} c_{-l} \, \nu[t+l] \right\} = \sum_{l=-\infty}^{\infty} c_l^* \, \nu[t-l]. \tag{17}$$

Therefore in the case of 1D metrology data, if ARMA modeling is successful, there is a corresponding TILF operator that describes the metrology result as a filtered white Gaussian noise. The identified TILF can be used for forecasting of a new slope distribution possessing the same statistical properties as the measured one, but with different parameters, such as the distribution length and the rms variation. A straightforward generalization of the 1D expressions (10)-(17) to the 2D case opens a way for parametrization and forecasting of 2D metrology data by applying 2D TILF modeling.

Note that there is a simple relation between the coefficients of the AR terms of Eq. (9) and the weights of a TILF that transforms the 'two-sided AR' process into the noise process $\nu[t]$. In some sense, such a TILF is the inverse operator to the one in Eq. (14). In this case, the AR part of Eq. (9) can be written as:

$$X[t] = \frac{1}{2} \sum_{l=-p}^{p} a_l \, X[t-l] - \frac{1}{2} a_0 \, X[t] + \nu^*[t], \tag{18}$$

with the coefficients a_l, $l = \pm 1, ..., \pm p$ determined by AR modeling the direct and the reversed traces of the same slope measurement. Assigning $a_0 = 0$, Eq. (18) is rewritten in a form of a TILF transformation:

$$\nu[t] = \sum_{l=-p}^{p} c_l \, X[t-l] - X[t] \equiv (C - I) * X[t], \tag{19}$$

where white Gaussian noise $\nu[t] = -\nu^*[t]$, I is the identity operator, and C a finite time-invariant linear filter of order p with the weights

$$c_l = a_l / 2, \text{ for } l = \pm 1, ..., \pm p, \text{ and } c_0 = 0, \text{ for } l = 0. \tag{20}$$

Filter C in expression (19), when applied to the process $X[t]$, gives a new stationary random process $Y[t]$ that differs from the process $X[t]$ by the noise process $\nu[t]$. If the difference is small (e.g., the variance of the noise is much smaller of that of the processes $X[t]$ and $Y[t]$), the TILF C can be thought as a good model of the stochastic process $X[t]$, representing its structure with the weight coefficients given by Eq. (20).

Practically, in order to determine a TILF filter C that best models the observed stochastic process $X[t]$, one has to find a set of the weight coefficients c_l that minimizes the deviation

$$E\left(\left[X[t]-Y[t]\right]^2\right)\equiv E\left(v^2[t]\right) \tag{21}$$

of the modeled process from the observed one.

3.2 Symmetry of TILFs for modeling of surface slope metrology

Generally, the values of the TILF weights with the same positive and negative lags are not necessarily equal, that is

$$c_l \neq c_{-l}\,. \tag{22}$$

However, as we mathematically prove in this section, among all TILFs (including AR and ARMA models) of the same order, the symmetrical filter with

$$c_l = c_{-l} \tag{23}$$

provides the smallest variance of the residual noise, which is equal to the difference between the measured trace and the best-fitted model. In the case of causal TILFs (like AR and ARMA models), it can be intuitively understood as a result of averaging of the residual noises of the fits with the corresponding causal filters of the direct and reversed processes. Assuming that the residual noises are not mutually correlated, one should expect a suppression of the variance of the averaged residual noise by a factor of two with respect to the corresponding causal filter.

For mathematical proof of the statement given with Eq. (23) we will show that replacement of a given TILF with its symmetric form reduces the variance of the difference between the observed and modeling stochastic processes.

Let us define

$$c_l = \overline{c}_l + \delta c_l \quad \text{and} \quad c_{-l} = \overline{c}_l - \delta c_l\,, \tag{24}$$

where $\overline{c}_l = (c_l + c_{-l})/2$ and $\delta c_l = (c_l - c_{-l})/2$ and $|l| \le p$, p is the order of the TILF model C. In these notations,

$$Y[t] = \sum_{k=1}^{p} \overline{c}_k \left[X[t-k] + X[t+k]\right] + \sum_{l=1}^{p} \delta c_l \left[X[t-l] - X[t+l]\right] \equiv u[t] + v[t]\,. \tag{25}$$

Therefore, the variance of the difference between $X[t]$ and $Y[t]$ is

$$\begin{aligned} E\left(\left[X[t]-Y[t]\right]^2\right) &= E\left(\left[X[t]-u[t]\right]^2\right) + E\left(v^2[t]\right) + \\ 2\sum_{l=1}^{p} \delta c_l E\left(\left\langle X[t] - \sum_{k=1}^{p} \overline{c}_l \left[X[t-k]+X[t+k]\right]\right\rangle \left[X[t-l]-X[t+l]\right]\right). \end{aligned} \tag{26}$$

Let us show that the last sum in (26) equals zero as each of its terms is zero. The elements in the sum are of two types (up to multipliers) that can be reduced to the auto-covariance function of the process $X[t]$:

$$E\left(X[t]\left[X[t-k]-X[t+k]\right]\right) = E\left(X[t]X[t-k]\right) - E\left(X[t]X[t+k]\right) = r_X[k] - r_X[-k] = 0 \tag{27a}$$

and

$$E\left(\left[X[t-k]+X[t+k]\right]\left[X[t-k]-X[t+k]\right]\right) = r_X[0] + r_X[2k] - r_X[2k] - r_X[0] = 0\,. \tag{27b}$$

Therefore, the variance of the difference between $X[t]$ and $Y[t]$ equals (compare with Eq. A3)

$$E\left(\left[X[t]-Y[t]\right]^2\right) = \sum_{n}\left[X[t] - \sum_{l=1}^{p} \overline{c}_l \left(X[t-l]+X[t+l]\right)\right]^2 + \sum_{l=1}^{p} \left(\delta c_l\right)^2 E\left[X[t-l]-X[t+l]\right]^2. \tag{28}$$

For a symmetrical filter with $c_l = c_{-l}$, the second sum is zero and the variance of the difference between $X[t]$ and $Y[t]$ is smaller than that of an asymmetrical one with $c_l \neq c_{-l}$.

4. EVALUATION OF THE BEST SYMMETRICAL TILF OF A GIVEN ORDER

Summarizing the above consideration, we describe 1D slope metrology with high quality x-ray mirrors as stochastic stationary processes $X[t]$ defined on a unit lattice $\mathbb{Z}^1$ (index 1 denotes one-dimensional integer lattice) and build corresponding symmetrical TILF models of an auto-regressive type. In AR TILF models, a value of a process at a given point t is approximated by a linear combination of values of the process at points within the vicinity. If the approximation achieved is accurate enough, one may say that the chosen model fits the original random process and can be used for parametrization of the metrology data, and therefore the polishing process used for fabrication of the mirrors. In particular, a power spectral density of the process can be approximated with the PSD of the model. With the weights of the model known, one can analytically evaluate the PSD function.

The key task is the identification of an optimal TILF that best models (with minimum number of parameters and with the smallest possible residual noise) the observed stationary stochastic process.

As discussed in Sec. 2.1 and in our previous publications,[10,11] we model surface slope measurements with a TILF, which is built based on symmetrization of the ARMA process, determined with EViews 8 software.[19] Here we present an original algorithm for direct optimization of the TILF model without involving results of the ARMA modeling.

Let C be a symmetric TILF of the order p defined with weight coefficients $c_1,\ldots,c_p$. In order to select the coefficients, one has to minimize the variance between the observed process $X[t]$ and the approximating one, $Y[t]$ [compare with Eq. (28) in Sec. 3.2]:

$$E\left(\left[X[t]-Y[t]\right]^2\right) = r_X[0] - 4\sum_{l=1}^{p} c_l\, r_X[l] + \sum_{k=1}^{p}\sum_{l=1}^{p} c_k\, c_l\, q[k,l], \tag{29}$$

where $q[k,l]$ are the elements of a $p\times p$ matrix Q, built of the coefficients for the auto-covariance function of the process $X[t]$:

$$q[k,l] \equiv r_X[k+l] + r_X[k-l] = r_X[|k+l|] + r_X[|k-l|]; \quad 1 \le k,\, l \le p. \tag{30}$$

Note that the matrix Q is symmetric: $Q = Q^T$.

By introducing the vectors of the TILF weights and the process auto-covariance:

$$\vec{c} \equiv \left\langle c_1,\ldots,c_p \right\rangle \text{ and } \vec{r}_X \equiv \left\langle r_X[1],\ldots,r_X[p] \right\rangle, \tag{31}$$

the variance equation (29) can be written in the matrix form:

$$E\left(\left[X[t]-Y[t]\right]^2\right) = r_X[0] - 4\vec{c}\,\vec{r}_X{}^T + 2\vec{c}\,Q\,\vec{c}^T. \tag{32}$$

The weight coefficients of the optimal symmetric TILF correspond to the minimum value of the variance in Eq. (32). Below we derive an analytical expression that allows determination of the optimal weight coefficients for the case where the inverse of matrix Q exists.

Let us add finite-difference derivative $\delta\vec{c}$ to vector $\vec{c}$: $\vec{c}+\delta\vec{c}$, $\delta\vec{c} << \vec{c}$, and insert the result to Eq. (32):

$$\delta E\left(\left[X[t]-Y[t]\right]^2\right) = -4(\vec{c}+\delta\vec{c})\,\vec{r}_X{}^T + 2(\vec{c}+\delta\vec{c})\,Q\,(\vec{c}+\delta\vec{c})^T + 4\vec{c}\,\vec{r}_X{}^T - 2\vec{c}\,Q\,\vec{c}^T. \tag{33}$$

By performing straightforward algebraic transformations and leaving in the right term only the part, linear with respect to $\delta\vec{c}$, Eq. (33) can be transformed to

$$\delta E\left(\left[X[t]-Y[t]\right]^2\right)=-4\,\delta\vec{c}\,\vec{r}_X{}^T+2\,\delta\vec{c}\,Q\,\vec{c}^{\,T}+2\,\vec{c}\,Q\,\delta\vec{c}^{\,T}=4\delta\vec{c}\left(-\vec{r}_X{}^T+Q\,\vec{c}^{\,T}\right). \tag{34}$$

In order to get (34), we use the facts that $\delta\vec{c}\,Q\,\vec{c}^{\,T}$ and $\vec{c}\,Q\,\delta\vec{c}^{\,T}$ are just constants and that the matrix Q is symmetric; therefore

$$\delta\vec{c}\,Q\,\vec{c}^{\,T}=\left(\delta\vec{c}\,Q\,\vec{c}^{\,T}\right)^T=\left(Q\,\vec{c}^{\,T}\right)^T\,\delta\vec{c}^{\,T}=\vec{c}\,Q^T\,\delta\vec{c}^{\,T}=\vec{c}\,Q\,\delta\vec{c}^{\,T}. \tag{35}$$

From (34), the variance between the observed process $X[t]$ and the approximating one, $Y[t]$ reaches its minimum at

$$\left(-\vec{r}_X{}^T+Q\,\vec{c}^{\,T}\right)=0,\ \text{that is}\ \vec{r}_X{}^T=Q\,\vec{c}^{\,T}\ \text{or}\ \vec{r}_X=\vec{c}\,Q\ . \tag{36}$$

If the inverse of matrix Q exists, one gets a condition for determining the weight coefficients of the optimal symmetric TILF:

$$\vec{c}=\vec{r}_X Q^{-1}. \tag{37}$$

In order to determine the minimum value achieved by the variance (32), we substitute condition (37) into (32):

$$\begin{aligned}E\left(\left[X[t]-Y[t]\right]^2\right)_{MIN}&=r_X[0]-4\vec{r}_X\,Q^{-1}\,\vec{r}_X{}^T+2\left(\vec{r}_X\,Q^{-1}\right)Q\left(\vec{r}_X\,Q^{-1}\right)^T\ldots\\&=r_X[0]-4\vec{r}_X Q^{-1}\,\vec{r}_X{}^T+2\vec{r}_X\left(Q^{-1}\right)^T\vec{r}_X{}^T.\end{aligned} \tag{38}$$

And finally, the expression for calculating the minimum value of the variance between the observed process $X[t]$ and the approximating one, $Y[t]$, is

$$E\left(\left[X[t]-Y[t]\right]^2\right)_{MIN}=r_X[0]-2\vec{r}_X\,Q^{-1}\,\vec{r}_X{}^T. \tag{39}$$

Equations (37) and (39) provide an algorithm for evaluation of the best TILF with given order p .

5. VERIFICATION OF THE DEVELOPED ALGORITHM FOR IDENTIFICATION OF OPTIMAL SYMMETRICAL TIME-INVARIANT LINEAR FILTER

In this section, we will verify the developed algorithm for determining weight coefficients of an optimal symmetrical TILF (Sec. 4) in application to modeling a series of stochastic processes, generated with the ARMA model[12,13] built from surface slope data, measured with the ALS DLTP[25] of the LCLS beam split and delay mirror.[30] The DLTP is capable of slope metrology for plane surfaces with absolute error better than 80 nrad and rms error less than 50 nrad.[31] The overall error of the used data is estimated to be less than 60 nrad (rms).

5.1 ARMA model for slope data measured with the LCLS beam split and delay mirror

Figure 1a (blue solid line) shows the residual (after subtraction of the best fit third polynomial) slope variation over the mirror clear aperture of 138 mm. The trace consists of *N*=691 points measured with an increment of $\Delta x=0.2$ mm.

The best fit slope trace, shown in Fig. 1a with the red dashed line, corresponds to the ARMA model specified in Table 1. The table, generated by EViews 8 software[19] as the regression output, only includes the statistically significant ARMA parameters.

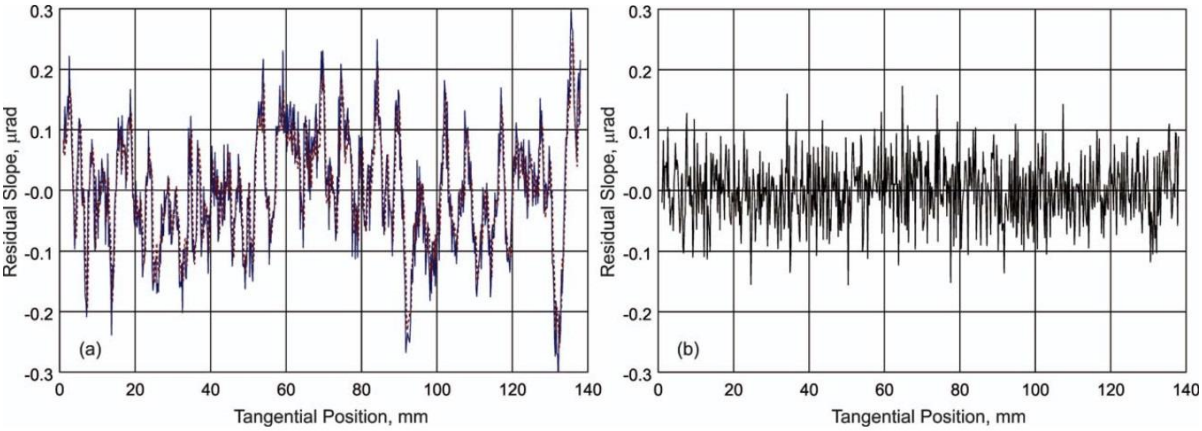

Figure 1: (a) Measured slope trace (the blue solid line) after subtracting the best-fit third polynomial shape in order to remove the trend that is characteristic for short x-ray mirrors; and best-fit slope trace (the red dashed line), corresponding to the ARMA model specified in Table 1. The rms variation of the measured slope trace is 0.099 µrad. (b) Difference between the measured and fitted traces. The rms variation of the slope difference is 0.053 µrad.

Table 1. Parameters of the ARMA model (the green solid line in Fig. 1a), which best fits the surface slope trace for the LCLS beam split and delay mirror measured with the ALS DLTP. In Eqs. (1-5), b_0=1 and σ^2 is equal to the standard error of the regression of 0.053 µrad (rms). The data are the regression outputs generated by EViews[19] software.

Variable	Coefficient	Standard Error
AR(1): a_1	0.637	0.036
AR(2): a_2	0.352	0.041
AR(5): a_5	-0.147	0.027
MA(2): b_2	- 0.0659	0.0035

The slope difference trace shown in Fig. 1b is the driving noise of the ARMA model that is $v[n]$ in Eq. (1). It should be distinguished from any observation noise or measurement error. The details of the ARMA modeling of the slope metrology with the LCLS beam split and delay mirror can be found in Refs.[12,13]

5.2 ARMA forecasting of surface topography for mirrors with 500 mm length, statistically identical to the LCLS split and delay mirror

The ARMA model established for the LCLS beam split and delay mirror and depicted in Table 1, was used to forecast a number of new surface slope distributions that can be thought of as the data for prospective mirrors, manufactured with the same polishing process at the fabrication facility of the real mirror modeled with ARMA.

Forecasting a new slope trace with the determined ARMA model is performed in two steps. First, we generate a new sequence of white-noise-like, normally distributed residuals $v[n]$ with a length of 500 mm (with 0.2-mm increment) corresponding to the new desired mirror length. Second, by using Eq. (1) with the ARMA parameters in Table 1, and the extended residuals, a new slope trace is generated and normalized to get the rms slope variation of 0.1 µrad. Using uncorrelated sets of residuals $v[n]$, a number of statistically independent (inherently non-correlating), but statistically identical (with the pre-determined ARMA parameters), are generated with the EViews 8 software.[19]

The blue solid line in Fig. 2a presents one of the slope distributions, Slope 09, forecast based on the described procedure and the ARMA model in Table 1. The best-fit slope trace corresponding to the ARMA model specified in Table 3 is shown in Fig. 2a with the red dashed line. By ARMA modeling the traces with EViews 8 in a similar manner to that described in Refs.,[8-13] we verify statistical identity of the generated slope traces to the used ARMA model.

Within the statistical uncertainty, AR parameters of the ARMA models, identified for the generated slope traces (see Table 2), are equal to those of the ARMA model of the measured slope trace.

However, variation of the MA(2) parameter values are very large. A comparison with the results of an ARMA fit for an individual trace (for example, Slope 09 in Table 3) suggests that, in general, these ARMA fits are not sensitive to the moving average term. In the case of trace Slope 09, the value of b_2 is larger than its error only by a factor of 1.5. Nevertheless, MA(2) term was kept in the parent ARMA model because it is needed to randomize the residuals of the ARMA fit for the measured slope trace in Fig. 1.

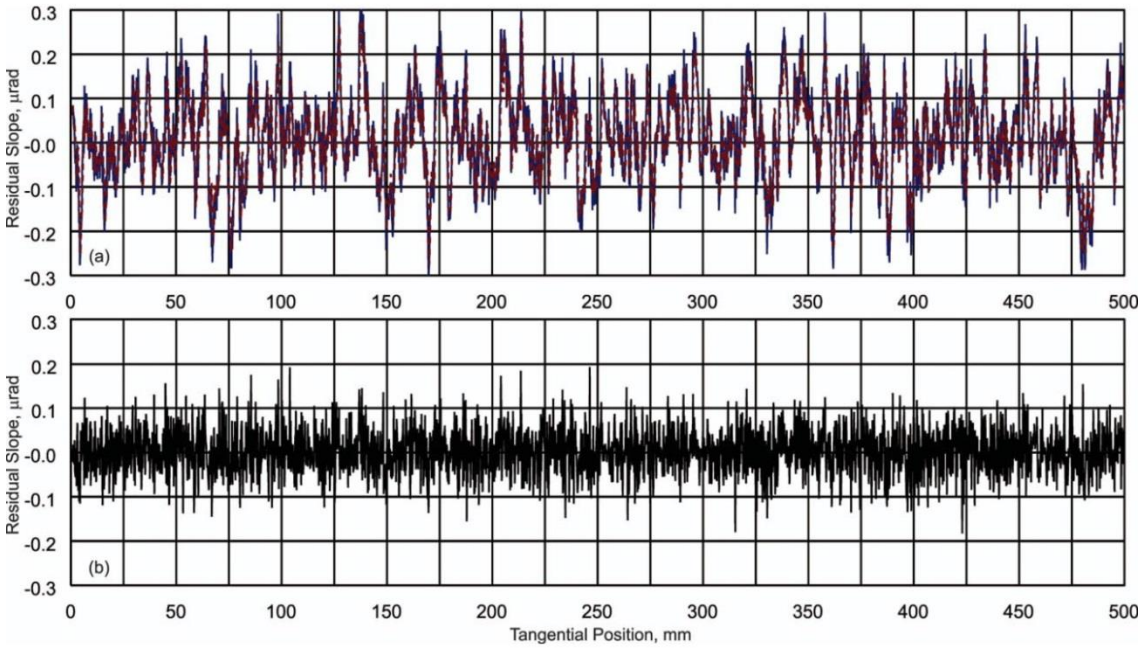

Figure 2: (a) Generated slope trace Slope 09 (the blue solid line) and best-fit slope trace (the red dashed line), corresponding to the ARMA model specified in Table 3. The rms variation of the generated slope trace is 0.101 µrad. (b) Difference between the generated and fitted traces. The rms variation of the slope difference is 0.0523 µrad.

Table 2. Parameters of the ARMA models, which best fits the surface slope traces generated with the parent ARMA model specified in Table 1. The values of the standard error of regression are given in micro-radians.

Trace\Parameter	a_1	a_2	a_5	b_2	**Standard Error of Regression**
Slope 01	0.6705	0.3008	-0.1512	-0.0041	0.0519 µrad
Slope 02	0.6362	0.3251	-0.1325	-0.0175	0.0523 µrad
Slope 03	0.6032	0.3737	-0.1545	-0.0376	0.0541 µrad
Slope 04	0.6517	0.3208	-0.1447	-0.0587	0.0524 µrad
Slope 05	0.6098	0.3805	-0.1556	-0.0950	0.0517 µrad
Slope 06	0.6936	0.1874	-0.0737	0.1624	0.0538 µrad
Slope 07	0.6166	0.4010	-0.1712	-0.1027	0.0531 µrad
Slope 08	0.6563	0.3244	-0.1349	-0.0560	0.0531 µrad
Slope 09	0.6378	0.3462	-0.1306	-0.0419	0.0523 µrad
Mean Value	0.6418	0.3289	-0.1388	-0.0279	0.0527 µrad
Standard Deviation	0.0296	0.0623	0.0277	0.0783	0.0008 µrad

Table 3. Parameters of the ARMA model (the green solid line in Fig. 2a), which best fits the generated surface slope trace Slope 09. In Eqs. (1-5), b_0=1 and σ^2 is equal to the standard error of the regression of 0.0523 µrad (rms). Note that the ARMA fit is not sensitive to the moving average term; the value of b_2 is larger than its error only by a factor of 1.5. The data are the regression outputs generated by EViews[19] software.

Variable	Coefficient	Standard Error
AR(1): a_1	0.6378	0.0197
AR(2): a_2	0.3462	0.0284
AR(5): a_5	-0.1306	0.0172
MA(2): b_2	-0.0419	0.0296

The generated slope traces, as the one shown in Fig. 2 and with the best fit ARMA parameters in Table 2, are used to test the developed algorithm for determining the TILF weight parameters.

5.3 AR-TILF filters with analytically derived weight coefficients for 1D data generated with the known ARMA model

Here, we investigate the performance of modeling the stochastic polishing process using symmetric TILFs and the developed analytical procedure for determining weight coefficients of the optimal filter. For this, we apply the calculation algorithm based on Eqs. (37) and (39) to fit nine slope traces generated with the known parent ARMA model as described in Secs. 5.1 and 5.2. Such generated traces are *a priori* the results of a uniform, stationary stochastic process; and therefore, they are ideal objects for testing the developed TILF-based modeling approach.

Figure 3 illustrates the TILF approximation of the same generated trace (Slope 09) as the one shown in Fig. 2 with its best ARMA fit. The blue solid line in Fig. 3 represents the generated slope trace. The optimal approximation with the developed symmetric TILF is depicted in Fig. 3a with the red dashed line.

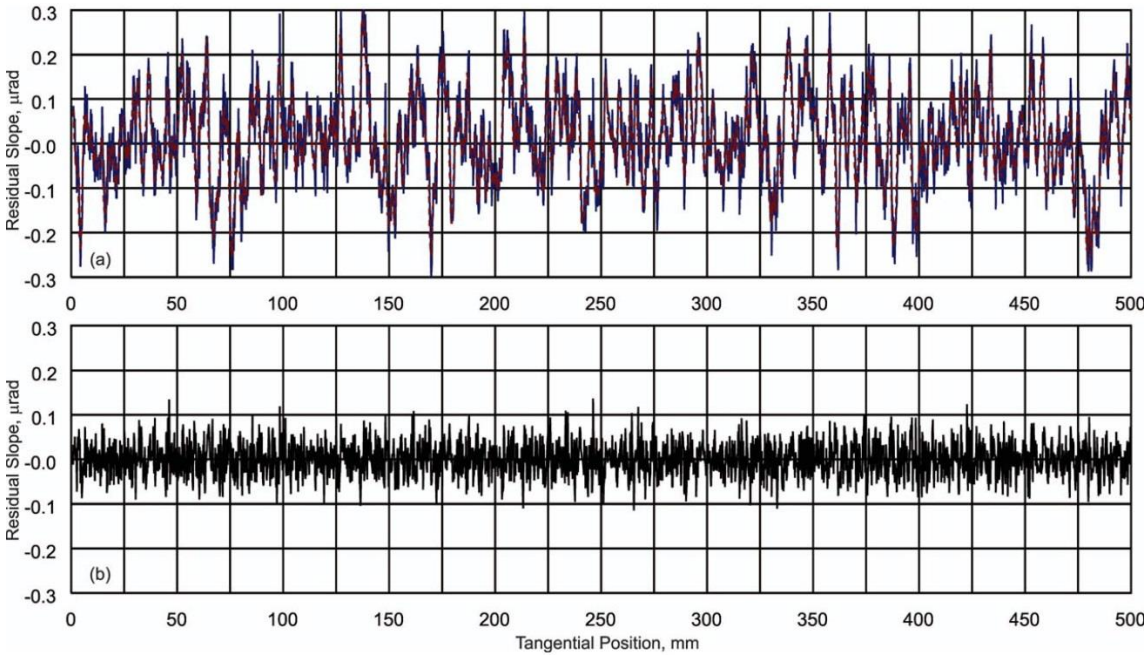

Figure 3: (a) Generated slope trace Slope 09 (the blue solid line) and the slope trace approximation (the red dashed line), obtained by application to the generated trace Slope 09 of the optimal symmetric TILF with the weight coefficients in Table 3, determined using the analytical procedure presented in Sec. 4. (b) Difference between the generated and fitted traces. The rms variation of the slope difference is 0.0380 µrad.

For modeling, we use symmetric TILF of order $p = 5$, corresponding to the AR order parameter p of the parent ARMA model. The question about the optimal number of coefficients is out of the scope of the present work and will be investigated elsewhere.

Table 4 presents the weight coefficients of the optimal symmetric TILF determined by application of the developed fitting procedure to nine slope traces generated with the parent ARMA model. The mean values of the coefficients estimated by averaging of nine coefficients with the same lag, as well as the standard deviation of the coefficients are shown in the last two rows of Table 4.

Table 4. Weight coefficients of the TILF models, which best fit the surface slope traces generated with the known parent ARMA model as described in Secs. 5.2 and 5.3.

Trace\Coefficient	c_1	c_2	c_3	c_4	c_5
Slope 01	0.3078	0.1892	0.0170	0.0753	-0.1009
Slope 02	0.2812	0.2005	0.0601	0.0435	-0.0993
Slope 03	0.2581	0.2124	0.0619	0.0710	-0.1165
Slope 04	0.3136	0.1582	0.0322	0.0865	-0.1012
Slope 05	0.2839	0.1742	0.0648	0.0673	-0.1019
Slope 06	0.3137	0.1427	0.0647	0.0525	-0.0798
Slope 07	0.2803	0.1711	0.0607	0.1007	-0.1230
Slope 08	0.3117	0.1588	0.0486	0.0799	-0.1113
Slope 09	0.2840	0.1898	0.0549	0.0510	-0.0886
Mean value	0.2927	0.1774	0.0517	0.0697	-0.1025
Standard Deviation	0.0197	0.0224	0.0166	0.0184	0.0133

Note that if we double the mean values of the TILF weight coefficients in Table 4, they will be close to the values of the corresponding (with the same lag) AR parameters of the parent ARMA model, given in Table 1. The small difference is probably due to the extra two fitting AR-like parameters in the TILF.

One of the major advantages of the developed TILF approximation is that the residual slope, calculated as a difference between the generated slope trace and the corresponding fit, has, as predicted (see Sec. 3.2), a smaller variation than the ARMA approximation. For the slope trace Slope 09, the improvement is about a factor of 1.38 , close to $\sqrt{2}$ (compare Fig. 2b and Fig. 3b).

The algorithm of approximation with symmetric TILF, developed in this paper, is based on analytical transformation of the auto-covariance function of the stochastic process under treatment [refer to Sec. 4 and Eqs. (37) and (39)]. Therefore, in our case it is natural to use, as a measure of fidelity of the TILF model, the difference between the ACFs of the generated trace and its TILF approximation. As a typical result, we illustrate the fidelity of the developed TILF modeling with the example of the generated trace Slope 09.

Figure 4 shows the ACFs of trace Slope 09 and its TILF approximation (Fig. 3a), as well as the difference of the ACFs. Almost over the entire range of lag values, except a very tiny central region, the difference has a clear random character. The regions of the ACFs in the central vicinity of lag $l = 0$ are depicted in Fig. 5 with enlarged scale. Here also there is a very close resemblance of the two ACFs, almost over the entire range of represented lags. This means that the two stochastic processes, generated and approximated, are spectrally close, and therefore, the determined TILF is highly accurate.

The ACF of the residual trace (Fig. 3b) that is the difference between the generated trace and its TILF approximation is shown in Fig. 6a. The delta-function-like ACF suggests for a white-noise-like character of the residual trace. For comparison, the ACF of a computer generated white-noise trace with the same value of the rms variation is depicted in Fig. 6b. The inset in Fig. 6 represents the difference of the ACFs in Fig. 6a and Fig. 6b, plotted with significantly larger scale.

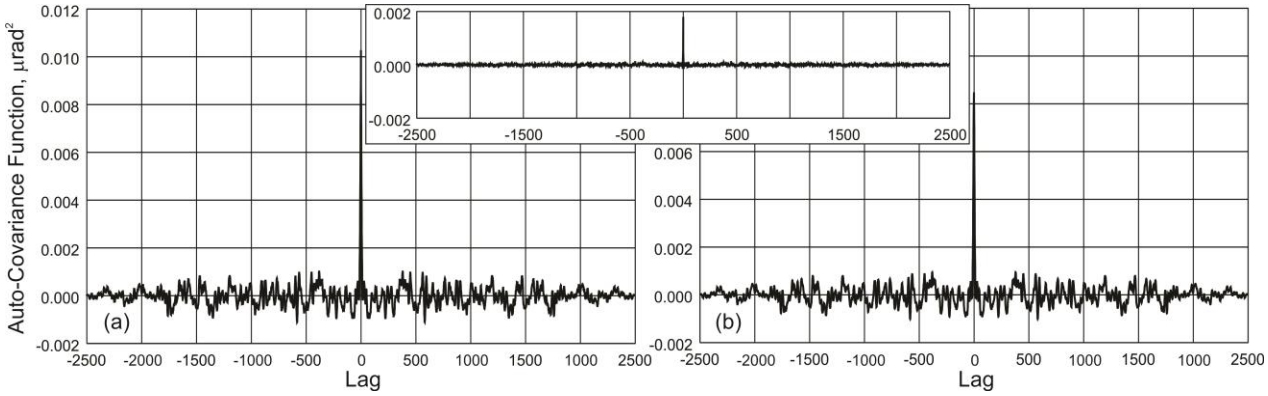

Figure 4: (a) ACF of the generated trace Slope 09 and (b) its TILF approximation. The inset shows the difference of the ACFs in plots (a) and (b). Except a very tiny central region, the difference has a clear random character, indicating high accuracy of the determined TILF.

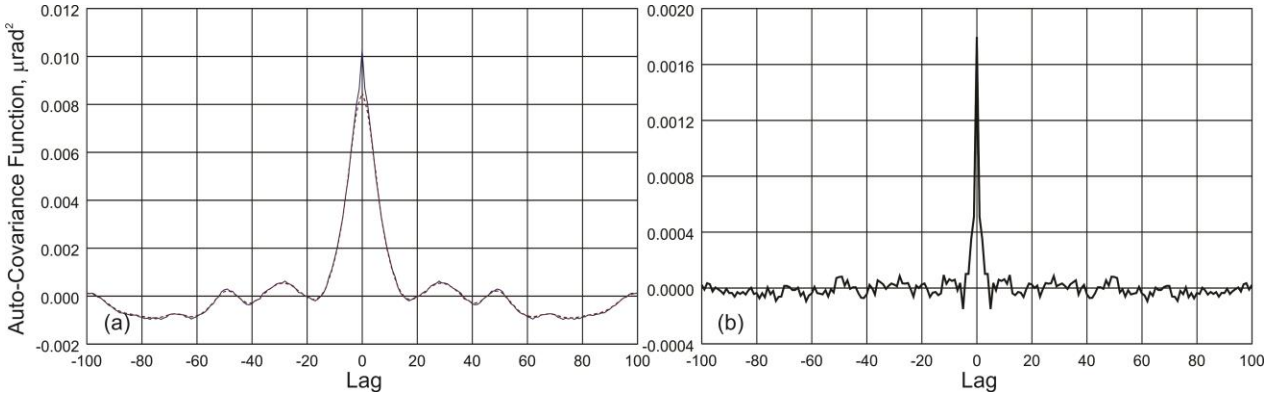

Figure 5: (a) Central regions of the ACFs of the generated trace Slope 09 (the blue solid line) and its TILF approximation (the red dashed line). (b) Difference between the ACFs of the generated and fitted traces in plot (a). Note that the vertical scale in (b) is increased by a factor of ~6.

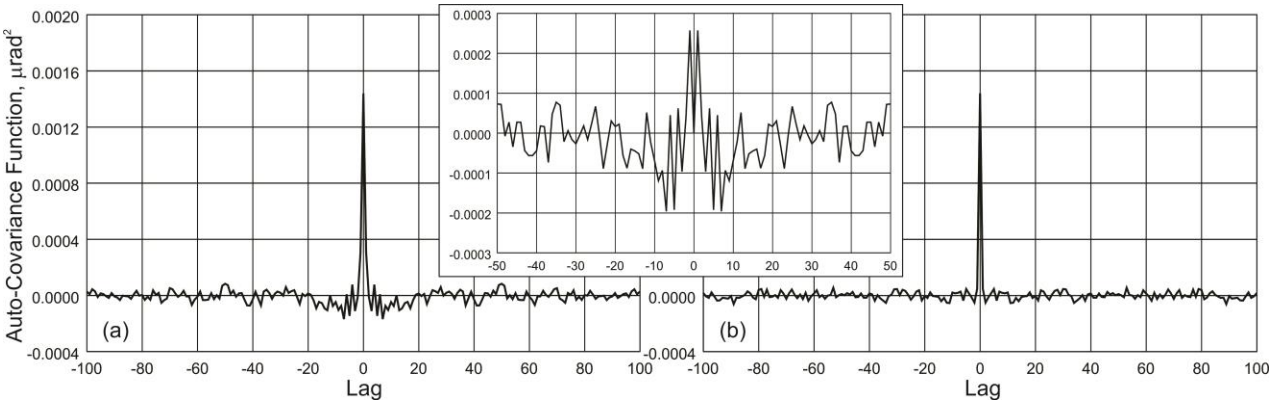

Figure 6: (a) Central regions of the ACF of the difference between the generated trace and its TILF approximation shown in Fig. 3b. (b) ACF of white noise trace with the same value of the rms variation. The inset shows the difference of the ACFs in plots (a) and (b). Note that the vertical scale in inset is increased by a factor of ~4.

The two-peak character of the ACF difference in Fig. 6 can be a signature of residual MA contributions to the stochastic process that are not approximated with the developed symmetric TILF model. However, ARMA modeling of the residual trace in Fig. 3b with EViews 8 software does not provide any reasonable model that would noticeably decrease the variance of the residual trace. This suggests for an almost perfect white-noise-like distribution of the residuals.

6. CONCLUSION

In this work, we have continued the investigation, started in Refs.,[8-11] that will potentially allow us to analytically characterize/parameterize the polishing capabilities of different vendors for x-ray optics. Based on the parametrization, the expected surface profiles of the prospective x-ray optics will be reliably simulated (forecast) prior to purchasing. The simulated surface slope and height distributions of prospective optics (before they are fabricated) can be used for estimations of the expected performance of new x-ray optical systems (beamlines, x-ray telescopes, etc.).[12,13]

We have analyzed a generalization of ARMA modeling with the TILF approach. We have analytically shown that the suggested symmetric TILF approximation has all the advantages of one-sided AR and ARMA modeling, along with improved fitting accuracy. It is also free of the causality problem, which can be thought of as a limitation of ARMA modeling of surface metrology data.

A new algorithm for identification of an optimal symmetric TILF with minimum number of parameters and smallest residual error has been derived. We have verified the efficiency of the developed algorithm in application to modeling of a series of stochastic processes, which were generated with the known ARMA model determined from surface slope data of a state-of-the-art x-ray mirror.

The major motivation of the performed investigation of TILF based modeling of surface metrology data is the possibility of a direct, straightforward generalization of TILF modeling to 2D random fields. Mathematical foundations of the generalization are well established.[29] However, its practical realization requires development of calculation algorithms and dedicated software for determination of the optimal TILF best-fit of measured 2D surface slope and height distributions. The optimization can be done in a standard way, consisting of searching for the optimal filter's weights by using, for example, a method similar to one developed in this work. For reliable TILF forecasting of new surface topography based on measured and fitted ones, the residual noise of the fit has to have a zero mean unit variance white Gaussian distribution. This is similar to the ARMA modeling, and therefore, the corresponding methods and criteria could be applied to the statistical analysis of TILF modeling in dedicated software under development.

The forthcoming investigations have to solve the question about uniqueness of the ARMA and TILF parametrizations for a certain polishing process. This can be performed, for example, by cross-comparing the ARMA and TILF models for different optics of identical fabrication. This work is also in progress.

ACKNOWLEDGEMENT

The authors are very grateful to Daniel J. Merthe, Nikolay A. Artemiev, and Daniele Cocco for help with high accuracy surface slope measurements of the LCLS beam split and delay mirror, and to Gary Centers and Wayne McKinney for very useful discussions. This work was supported in part by NASA Small Business Innovation Research SBIR grant to Second Star Algonumerics, project No. 15-1 S2.04-9193. The Advanced Light Source is supported by the Director, Office of Science, Office of Basic Energy Sciences, Material Science Division, of the U.S. Department of Energy under Contract No. DE-AC02-05CH11231 at Lawrence Berkeley National Laboratory.

REFERENCES

[1] Assoufid, L., Hignette, O., Howells, M., Irick, S., Lammert, H., and Takacs, P., "Future metrology needs for synchrotron radiation grazing-incidence optics," Nucl. Instrum. Methods A 467-468, 267-70 (2001).
[2] Yamauchi, K., Yumamura, K., Mimura, H., Sano, Y., Saito, A., Kanaoka, M., Endo, K., Souvorov, A., Yabashi, M., Tamasaku, K., Ishikawa, Y., and Mori, Y., "Wave-optical analysis of sub-micron focusing of hard x-ray beams by reflective optics," Proc. SPIE 4782, 271-276 (2002).

[3] Samoylova, L., Sinn, H., Siewert, F., Mimura, H., Yamauchi, K., and Tschentscher, T., "Requirements on Hard X-ray Grazing Incidence Optics for European XFEL: Analysis and Simulation of Wavefront Transformations," Proc. SPIE 7360, 73600E-1-9 (2009).
[4] Moeller, S., Arthur, J., Brachmann, A., Coffee, R., Decker, F.-J., Ding, Y., Dowell, D., Edstrom, S., Emma, P., Feng, Y., Fisher, A., Frisch, J., Galayda, J., Gilevich, S., Hastings, J., Hays, G., Hering, P., Huang, Z., Iverson, R., Krzywinski, J., Lewis, S., Loos, H., Messerschmidt, M., Miahnahri, A., Nuhn, H.-D., Ratner, D., Rzepiela, J., Schultz, D., Smith, T., Stefan, P., Tompkins, H., Turner, J., Welch, J., White, B., Wu, J., Yocky, G., Bionta, R., Ables, E., Abraham, B., Gardener, C., Fong, K., Friedrich, S., Hau-Riege, S., Kishiyama, K., McCarville, T., McMahon, D., McKernan, M., Ott, L., Pivovaroff, M., Robinson, J., Ryutov, D., Shen, S., Soufli, R., and Pile, G., "Photon beamlines and diagnostics at LCLS," Nucl. Instrum. and Methods A 635(1-1S), S6-S11 (2011).
[5] Idir, M., and Yashchuk, V. V., Co-Chairs, "Optical and X-ray metrology," in: X-ray Optics for BES Light Source Facilities, Report of the Basic Energy Sciences Workshop on X-ray Optics for BES Light Source Facilities, D. Mills and H. Padmore, Co-Chairs, pp. 44-55, U.S. Department of Energy, Office of Science, Potomac, MD (March 27-29, 2013); <http://science.energy.gov/~/media/bes/pdf/reports/files/BES_XRay_Optics_rpt.pdf> accessed: February 10, 2015.
[6] Gaskin, J. A., Weisskopf, M. C., Vikhlinin, A., et al., "The X-Ray Surveyor mission: A concept study," Proc. SPIE 9601, 96010J -1-14 (2015) [doi:10.1117/12.2190837].
[7] Yashchuk, V. V., Artemiev, N. A., Lacey, I., and Merthe, D. J., "Correlation analysis of surface slope metrology measurements of high quality x-ray optics," Proc. SPIE 8848, 88480I-1-15 (2013) [doi: 10.1117/12.2024694].
[8] Yashchuk, Y. V. and Yashchuk, V. V., "Reliable before-fabrication forecasting of expected surface slope distributions for x-ray optics," Opt. Eng. 51(4), 046501-1-15 (2012).
[9] Yashchuk, Y. V. and Yashchuk, V. V., "Reliable before-fabrication forecasting of expected surface slope distributions for x-ray optics," Proc. SPIE 8141, 81410N-1-15 (2011).
[10] Yashchuk, V. V., Tyurin, Y. N., and Tyurina, A. Y., "Application of the time-invariant linear filter approximation to parametrization of surface metrology with high-quality x-ray optics," Opt. Eng. 53(8), 084102 (2014).
[11] Yashchuk, V. V., Tyurin, Y. N., and Tyurina, A. Y., "Application of time-invariant linear filter approximation to parameterization of one- and two-dimensional surface metrology with high quality x-ray optics," Proc. SPIE 8848, 88480H-1-13 (2013).
[12] Yashchuk, V. V., Samoylova, L., and Kozhevnikov, I. V., "Specification of x-ray mirrors in terms of system performance: new twist to an old plot," Opt. Eng., 54(2), 025108 (2015).
[13] Yashchuk, V. V., Samoylova, L., and Kozhevnikov, I. V., "Specification of x-ray mirrors in terms of system performance: A new twist to an old plot," Proc. SPIE 9209, 92090F/1-19 (2014).
[14] Kay, S. M., [Modern Spectral Estimation: Theory and Application], Prentice Hall, Englewood Cliffs (1988).
[15] Jenkins, G. M. and Watts, D. G., [Spectral Analysis and its Applications], Fifth Printing: Emerson-Adams Press, Boca Raton (2007).
[16] Rasigni, G., Lafraxo, M., Buat, V., Rasigni, M., Abdellani, F., and Llebaria, A., "Autoregressive process for characterizing statistically rough surfaces," J. Opt. Soc. Am. A10(6), 1257-1262 (1993).
[17] Chen, B.-S., Lee, B.-K., and Peng, S.-C., "Maximum Likelihood Parameter Estimation of F-ARIMA Processes Using the Genetic Algorithm in the Frequency Domain," IEEE Trans. on Signal Processing 50(9), 2208-2219 (2002).
[18] Chang, S. Y. and Wu, H-C., "Novel Fast Computation Algorithm of the Second-Order Statistics for Autoregressive Moving-Average Processes," IEEE Trans. on Signal Processing 57(2), 526-535 (2009).
[19] [EViews 8 Software], http://www.eviews.com/home.html
[20] Popova, V. L. and Filippov, A. É., "A model of mechanical polishing in the presence of a lubricant," Tech. Phys. Lett. 31(9), 788–792 (2005).
[21] Pandit, S. M., Suratkar, P. T., and Wu, S. M., "Mathematical Model of a Ground Surface Profile with the Grinding Process as a Feedback System," Wear 39(2), 205-12 (1976).
[22] Fukumoto, I. and Ayabe, T., "Improvement of Ground Surface Roughness in Al-Si Alloys," Wear 137, 199-209 (1990).
[23] Rommeveaux, A., Thomasset, M., Cocco, D., Siewert, F., "First report on a European round robin for slope measuring profilers," Proc. SPIE 5921, 592101 (2005).
[24] Siewert, F., Assoufid, L., Cocco, D., Hignette, O., Irick, S., Lammert, H., McKinney, W., Ohashi, H., Polack, F., Qian, S., Rah, S., Rommeveaux, A., Schönherr, V., Sostero, G., Takacs, P., Thomasset, M., Yamauchi, K., Yashchuk, V., and Zeschke, T., [in: CD Proceedings of the AIP Conference on Synchrotron Radiation Instrumentation SRI-2006, III Workshop on Optical Metrology], Daegu, South Korea, May 27 - June 03 (2006).

[25] Yashchuk, V. V., Barber, S., Domning, E. E., Kirschman, J. L., Morrison, G. Y., Smith, B. V., Siewert, F., Zeschke, T., Geckeler, R., and Just, A., "Sub-microradian surface slope metrology with the ALS Developmental Long Trace Profiler," Nucl. Instrum. and Methods A 616(2-3), 212-223 (2010).
[26] Siewert, F., Noll, T., Schlegel, T., Zeschke, T., and Lammert, H., "The Nanometer Optical Component Measuring machine: a new Sub-nm Topography Measuring Device for X-ray Optics at BESSY," AIP Conference Proceedings 705, American Institute of Physics, Mellville, NY (2004), pp. 847-850.
[27] Siewert, F., Lammert, H., and Zeschke, T., "The Nanometer Optical Component Measuring Machine;" in: [Modern Developments in X-Ray and Neutron Optics], Edited by A. Erko, M. Idir, T. Krist, and A. G. Michette, Springer, New York (2008).
[28] Siewert, F., Buchheim, J., and Zeschke, T., "Characterization and calibration of 2nd generation slope measuring profiler," Nucl. Instrum. and Methods A 616(2-3), 119-127 (2010).
[29] Brockwell, P. J. and Davis, R. A., [Time Series: Theory and Methods], Second Ed., Springer, New York (2006).
[30] Murphy, B., "X-ray split and delay mirrors specifications," LCLS, 02/16/11: Drawings PF-391-946-11 and SA-391-946-13.
[31] Yashchuk, V. V., Artemiev, N. A., Lacey, I., McKinney, W. R., and Padmore, H. A., "A new x-ray optics laboratory (XROL) at the ALS: Mission, arrangement, metrology capabilities, performance, and future plans," Proc. SPIE 9206, 92060I -1-19 (2014) [doi:10.1117/12.2062042].